

# EFFECTS OF CALCINATION ON ELECTROPHORETIC DEPOSITION OF NATURALLY DERIVED AND CHEMICALLY SYNTHESIZED HYDROXYAPATITE

Onder Albayrak<sup>1</sup>, Cinar Oncel<sup>2</sup>, Mustafa Tefek<sup>3</sup> and Sabri Altintas<sup>1</sup>

<sup>1</sup>Department of Mechanical Engineering, Bogazici University, Bebek, 34342, Istanbul, Turkey

<sup>2</sup>Department of Material Science and Engineering, Sabanci University, Tuzla, 34956, Istanbul, Turkey

<sup>3</sup>Mersin Vocational School, Mersin University, 33343, Mersin, Turkey

Received: January 22, 2007

**Abstract.** In this study, electrophoretic deposition (EPD) method was used for hydroxyapatite (HA) coating on titanium substrates. Chemically synthesized nano-powders and naturally derived sub-micron powders of HA were produced and used as coating materials before and after calcination. Obtained coatings were sintered at 1000 °C for 1 hour. Besides HA coating, two applications including TiO<sub>2</sub> were performed: HA/TiO<sub>2</sub> composite coating in the one hand, and TiO<sub>2</sub> inner coating layer between titanium substrate and HA coating in the other. Results showed that, plate-like shaped nanosized HA powders with aspect ratio 3:1 were produced by the acid-base method. Ensuing calcination altered particle size (slightly coarsening) and shape (nodular-like). Coatings obtained using calcinated powders produced through acid-base method were seen to be free of cracks before and after sintering.

## 1. INTRODUCTION

Hydroxyapatite (HA), Ca<sub>10</sub>(PO<sub>4</sub>)<sub>6</sub>(OH)<sub>2</sub>, has been widely used in medical and dental applications such as dental implants, alveolar bridge augmentation, orthopedics, maxillofacial surgery and drug delivery systems due to its close similarity in chemical composition and high biocompatibility with natural bone tissue [1].

Although a number of ceramic and chemistry based processing routes have been developed for synthesizing nanosized HA and sintering of the powders, it is difficult to produce high purity HA because calcium phosphates have many derivatives and the synthesis of calcium phosphates strongly depends on reaction conditions [2]. Most

commonly used techniques for HA formation are precipitation, solid state reaction, sol-gel methods, hydrothermal route, emulsion and microemulsion techniques, mechanochemical reaction and ultrasonically assisted reaction [2,3]. The wet chemical process, which is based on precipitation route, is the most convenient and commonly used process [2,3]. The most widely used precipitation method is the acid-base method which is suitable for an industrial production of HA since the reaction involves no foreign element and the only by-product is water [2,4].

Application of HA in the human body has been limited due to its poor mechanical properties [5]. Unlike HA, titanium alloys are proven to be potentially very suitable materials for load bearing

---

Corresponding author: Onder Albayrak, e-mail: ondera@boun.edu.tr

bioimplant applications [6]. The concept of coating metal implant surfaces with HA combines the mechanical benefits of metal alloys with the biocompatibility of HA. Coating biologically inert metallic implants with biologically active materials, like HA, is an attempt to accelerate bone formation on initial stages of osseointegration, thus improving implant fixation [6,7].

Many coating techniques have been employed for the preparation of HA coatings, such as plasma spraying, dip coating, chemical solution deposition, sputter coating, biomimetic coating and electrophoresis [5,8,9]. The electrophoretic process exhibits some advantages over other alternative processes, such as simplicity in setup, low equipment cost and the capability to form complex shapes and patterns [6,10]. A high degree of control of coating deposit morphology can be obtained by adjusting deposition conditions and the ceramic powder size and shape [8]. Besides these advantages, ceramic coatings on metallic substrates present problems such as the appearance of cracks on coating surfaces after the process of deposit, drying and sintering [8].

Although HA is useful for absorption of bacteria, virus, ammonia and organic materials, it cannot decompose organic materials which are absorbed [11]. Contrary to HA,  $\text{TiO}_2$  photocatalyst can decompose organic materials and bacteria, which exist only on the surface of  $\text{TiO}_2$  [11]. In order to combine the advantages of HA and  $\text{TiO}_2$ , the ability of both absorption and decomposition of the harmful chemicals, HA coatings on  $\text{TiO}_2$  thin films have been developed [11].

In the present work, naturally derived (from calf femur) and chemically synthesized (through precipitation method) HA powders were produced and used in the electrophoretic deposition (EPD) as coating material; and effects of obtained powders (uncalcinated and calcinated) on coating efficiency were investigated. Besides HA coating, HA/ $\text{TiO}_2$  composite coating layer (to combine the advantages of HA and  $\text{TiO}_2$ ) and  $\text{TiO}_2$  inner coating layer (to prevent the in-vivo release of metal ions from the implants) were obtained by using EPD method.

## 2. EXPERIMENTAL

### 2.1. Production of HA powders

In this study, acid-base method was used to synthesize HA powders chemically and the procedure described by Wei [12] was followed. 5.0 g of  $\text{Ca}(\text{OH})_2$  (~99%, Merck, Germany) was dissolved

in 200 ml of deionized water using a magnetic stirrer. 4.669 g of liquid  $\text{H}_3\text{PO}_4$  (85%, Merck, Germany) was added slowly (to maintain  $\text{pH} > 9.5-10$ ) to the  $\text{Ca}(\text{OH})_2$  solution while the solution was continuously stirred by the magnetic stirrer. The pH value of the solution was continuously monitored using a pH meter (Orion 4 star model, Thermo, USA). Stirring was continued for 24 hours after  $\text{H}_3\text{PO}_4$  addition. Then centrifugation, supernatant decantation and resuspension in deionized water were applied 5 times. Obtained precipitates were oven-dried at  $80^\circ\text{C}$  for 24 hours. Half of obtained powders were calcinated in air atmosphere at  $1000^\circ\text{C}$  for 1 hour (heating rate of  $300^\circ\text{C}/\text{hour}$ ), followed by light grinding by hand with an agate mortar and pestle for 10 minutes. Dried and calcinated powders were coded as "1D" and "1C", respectively. Code "1" is used to specify precipitation method.

Naturally derived HA powders were obtained from calf femoral bones. Bones were boiled, attached to a mangle and cut with a hand saw, both ends were cut, bone marrow was extracted and bones were cleaned from all soft tissues attached to them; middle part of the femur was taken and cut into four pieces and each of these circular pieces cut further into four [13,14]. These pieces were heated to  $850^\circ\text{C}$  for 4 hours for complete removal of organic phases, and then were calcinated in air atmosphere at  $1000^\circ\text{C}$  for 1 hour (heating rate of  $300^\circ\text{C}/\text{hour}$ ), followed by light grinding by hand with an agate mortar and pestle for 10 minutes. These powders were coded as "2C" to specify naturally derived and calcinated samples.

### 2.2. Electrophoretic deposition

Obtained uncalcinated and calcinated HA powders were used as coating material. 0.5 g of powders was added into 80 ml ethanol (96%, Merck, Germany). After magnetically stirring for 15 minutes, suspensions were dispersed ultrasonically for 30 minutes at 40 kHz in an ultrasonic bath (Everest Elektromekanik, Turkey), and then suspensions were left to rest for 30 minutes to eliminate, by sedimentation, the bigger or agglomerated particles. Finally suspensions were ultrasonically dispersed again for 30 minutes to ensure a good dispersion of the particles [15,16].

Titanium substrates of  $15 \times 25 \times 1.5$  mm size were polished from 240 to 1000 grid SiC papers followed by using a  $1 \mu\text{m}$  diamond paste to get a mirror finish. Before deposition, substrates were thoroughly washed with detergent in ultrasonic bath for 30 minutes, followed by washing in acetone (extra

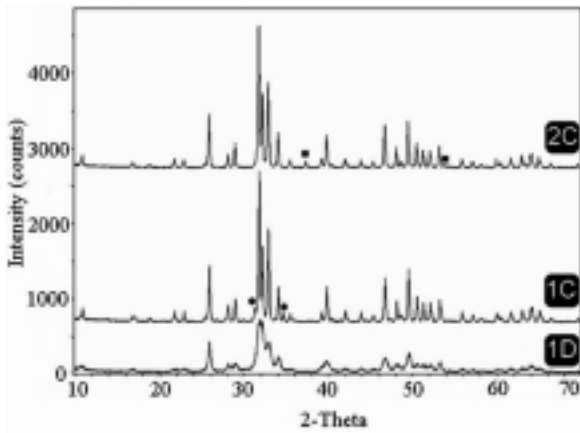


**Fig. 1.** XRD spectra of all obtained powders. ■ and ● are used for CaO and TCP, respectively. All other unsigned peaks are HA (1D: chemically synthesized dried powders; 1C: chemically synthesized calcinated powders; 2C: naturally derived calcinated powders).

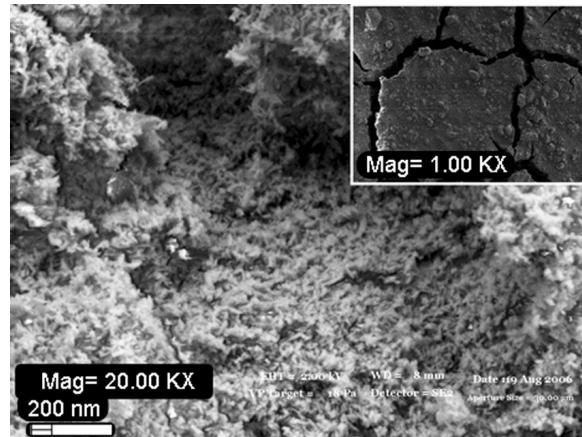


**Fig. 2.** SEM micrograph of dried HA nanoparticles produced by acid base method ( $\times 20,000$ ); top-right corner: SEM pictures of the HA deposits, using powders coded "1D", before sintering process ( $\times 1,000$ ).

pure, Merck, Germany) for another 20 minutes, and then passivated in 25 vol.% nitric acid (65%, Merck, Germany) overnight, then washed in distilled water [8,12].

pH values of the suspensions were adjusted in the range of 3-5 according to their zeta potential analysis results. At this stage, HA particles acquired positive charge and their deposition occurred at the cathode. The titanium electrodes were placed parallel to each other in the suspension, with a separation of 10 mm approximately, and connected to a d.c. power supply (Model AE-8150, Atto, Japan). The EPD process was performed under a constant voltage of 50 V for 1 minute. After deposition, the green form coatings were dried at room temperature in air, and then sintered in the tube furnace at 1000 °C for 1 hour in argon atmosphere at a heating rate of 100 °C/hour and cooling rate of 50 °C/hour. Same procedure was used for TiO<sub>2</sub> coatings by EPD. In these studies, commercially obtained (Alfa Aesar, Germany) nodular-shape, anatase form of TiO<sub>2</sub> with the particle size of 30-40 nm was used without any heat treatment before and after deposition.

### 2.3. Characterization

The phase purity and constitution of the synthesized powders were checked by powder X-ray diffractometry (XRD) (Model D/Max-Ultima+PC,

Rigaku, Japan). The XRD data were collected at a room temperature over the  $2\theta$  range of 10° - 70° at a step size of 0.02° and a count time of 0.6 sec.

Zeta potential analysis (Model Nano-ZS, Malvern, England) were performed in the pH range of 3-12 to determine the proper pH value used at the electrophoretic deposition. NaOH and HCl were used for pH adjustment; and ethanol was used as dispersant.

The morphology and particle size of the obtained HA powders and the morphology of the coating layers were observed by using SEM (Model Supra 35VP, Leo, Germany) at an accelerating voltage of 2 kV. Prior to SEM examination, all the samples were dried at 80 °C overnight, and sputter coated by carbon to minimize any possible surface charging effects. The images were obtained for the uncalcinated and calcinated powders as well as coating layer before and after sintering stage.

Scanning electron microscopy - energy dispersive X-ray (SEM-EDX) analysis and EDX mapping were performed to visualize the TiO<sub>2</sub> inner layer between titanium substrate and HA layer. EDX mapping was also used to illustrate the HA/TiO<sub>2</sub> composite coating layer.

## 3. RESULTS AND DISCUSSION

XRD spectra and results of phase identification for dried and calcinated powders are presented in Fig.

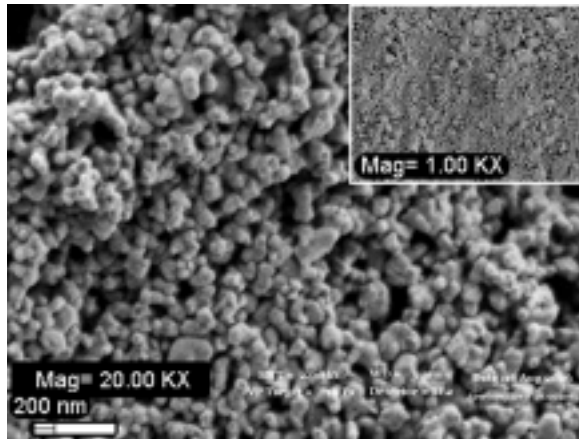


**Fig. 3.** SEM micrograph of calcinated HA nanoparticles produced by the acid base method ( $\times 20,000$ ); top-right corner: SEM pictures of the HA deposits, using powders coded “1C”, before sintering process ( $\times 1,000$ ).

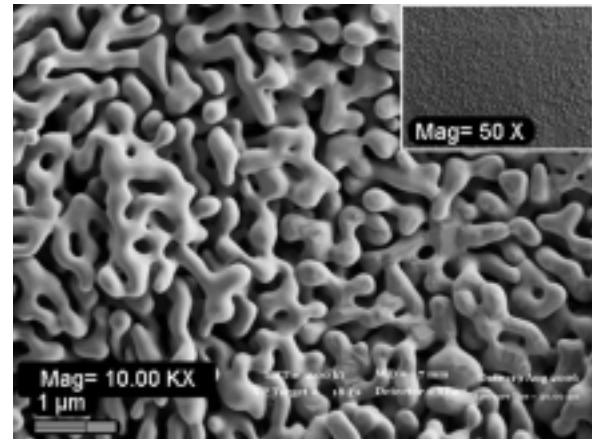


**Fig. 4.** SEM picture of the HA deposits, using powders coded “1D”, after sintering process ( $\times 10,000$ ); top-right corner: SEM pictures of the HA deposits, using powders coded “1C”, after sintering process ( $\times 50$ ).

1. Codes “1, 2, D, C” are used for chemically synthesized, naturally derived, dried and calcinated powders, respectively. Heating of the dried powders in air atmosphere at  $1000\text{ }^{\circ}\text{C}$  for 1 hour caused them to crystallize (Fig. 1). The observed phases in the “1D” coded chemically synthesized dried powders were determined by powder XRD to be completely HA (International Centre of Diffraction Data (ICDD), Powder Diffraction File (PDF) No: 84-1998). For the calcinated powders, besides primarily HA peaks, there were only a few peaks of tricalcium phosphate (TCP),  $\text{Ca}_3(\text{PO}_4)_2$  and calcium oxide (CaO) for the samples coded “1C” and “2C”, respectively.

SEM micrograph of dried powders that were chemically precipitated by acid-base method is shown in Fig. 2 revealing that the acid-base method produced plate-like nano-particles ( $\sim 120\text{ nm}$  by  $\sim 40\text{ nm}$ , aspect ratio  $\sim 3:1$ ). Further calcination of these particles at  $1000\text{ }^{\circ}\text{C}$  for 1 hour, coarsened them into nodular-like particles ( $\sim 180\text{ nm}$  by  $\sim 150\text{ nm}$ , aspect ratio  $\sim 1.2:1$ ) (Fig. 3).

Produced uncalcinated and calcinated HA powders were used to prepare suspension for EPD. To determine the proper pH value for EPD zeta potential analysis were performed, and zeta potentials as a function of pH for all HA/ethanol suspensions were obtained. Zeta potential values of all samples were over  $30\text{ mV}$  for the pH range of 3-5. Since high absolute zeta potential value indicates the presence of a well-dispersed suspension

[17], pH values of all suspensions were adjusted to approximately 4 to investigate the calcination effects on EPD.

The effects of calcination on coating characteristics (before sintering) are shown in the SEM micrographs of Fig. 2 and Fig. 3 revealing that, while the usage of uncalcinated powders at EPD caused cracks on coating surface (Fig. 2, top-right corner), calcinated powders exhibits crack-free surfaces (Fig. 3, top-right corner) even after sintering stage (Fig. 4, top-right corner). SEM micrograph of the sintered coating surface at  $1000\text{ }^{\circ}\text{C}$  for 1 hour (Fig. 4) presented apparent necking among the particles.

Cracks seen in Fig. 2 (top-right corner) arise as a result of shrinkage during drying. Drying shrinkage is minimized by the use of regularly shaped particles that can pack efficiently, large particle size distributions for gap-graded efficient packing, and large particle sizes [12]. Fig. 2 shows that cracking susceptibility appear to be dependent on the shape and size of the HA particles.

Finally, EPD containing  $\text{TiO}_2$  inner coating layer between titanium substrate and HA layer, and HA/ $\text{TiO}_2$  composite coating process were carried out. Although porous oxidation layer, with thickness of  $\sim 7\text{ }\mu\text{m}$ , was clearly observed on the surface of titanium after sintering process conducted in high purity argon atmosphere, it cannot prevent the ion transfer from titanium to HA [8].  $\text{TiO}_2$  inner coating layer was used not only to act as a chemical barrier against the release of metal ions from the im-

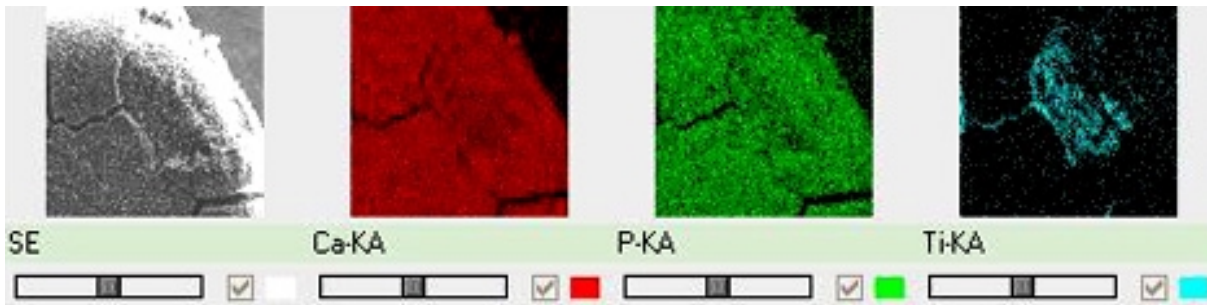


**Fig. 5.** SEM-EDX mapping to illustrate  $\text{TiO}_2$  inner layer.

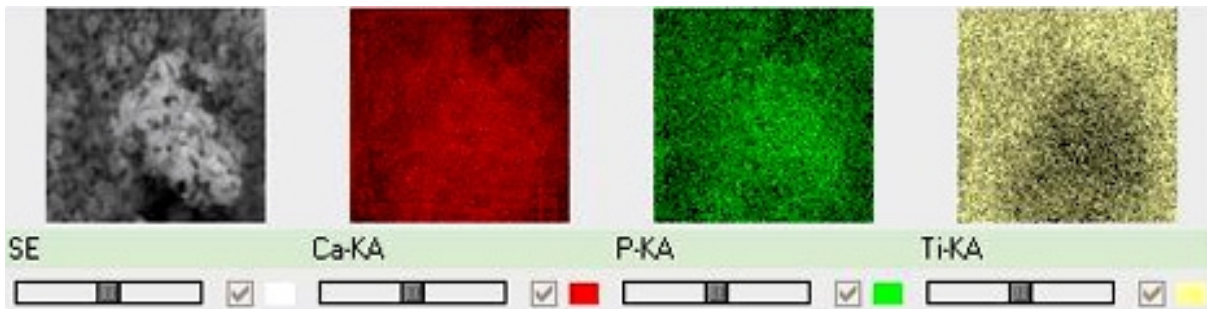


**Fig. 6.** SEM-EDX mapping to illustrate HA/ $\text{TiO}_2$  composite coating.

plant, but also to provide a chemical bonding between the titanium substrate and the HA coating in order to increase the adhesion strength. Besides, HA/ $\text{TiO}_2$  composite coating was expected to have the ability of both absorption and decomposition of harmful chemicals under UV irradiation. SEM-EDX mapping of  $\text{TiO}_2$  inner layer between titanium substrate and HA layer (Fig. 5) and HA/ $\text{TiO}_2$  composite coating (Fig. 6) were used to show the appearance of Ca, P and Ti in coating. At the application of  $\text{TiO}_2$  inner coating layer, spalling and cracking were observed on HA layer as shown in Fig. 5. At the study of HA/ $\text{TiO}_2$  composite coating 50:50 ratio were used and slightly cracks were observed. Thickness of these coating layers was about 20-30  $\mu\text{m}$  as obtained by electron microscopy of spalled parts.

#### 4. CONCLUSIONS

- XRD peaks of the precipitated dried powders at 80  $^\circ\text{C}$  for 24 hours, produced by acid-base method, completely match with the HA peaks (ICDD PDF No: 84-1998), no other phases are observed. Calcinating chemically precipitated and naturally derived HA powders at 1000  $^\circ\text{C}$  for 1 hour induces very high intensity of HA dif-

fraction peaks together with minor TCP and CaO peaks, respectively; and increases crystallinity.

- HA nano-particles produced by the acid-base method, dried at 80  $^\circ\text{C}$  for 24 hours, exhibit plate-like shapes ( $\sim 120$  nm by  $\sim 40$  nm) with an approximate aspect ratio of 3:1. After calcination at 1000  $^\circ\text{C}$  for 1 hour, these particles are observed to slightly coarsen and shapes of them turn to nodular-like ( $\sim 180$  nm by  $\sim 150$  nm) with an approximate aspect ratio of 1.2:1.
- The usage of uncalcinated powders at EPD caused cracks on coating surface, while calcinated powders exhibits crack-free surfaces even after sintering stage. The cracking susceptibility appears to correlate with particle shape: the more regular the particle shape (the closer it is to equal-axed), the less the cracking susceptibility.
- $\text{TiO}_2$  inner coating layer and HA/ $\text{TiO}_2$  composite coating were studied by using EPD. Although SEM-EDX and EDX mapping analysis illustrate that intended coatings were obtained, cracks were observed for both of them. Research is under way for the preparation of crack-free  $\text{TiO}_2$  based coatings.

## ACKNOWLEDGEMENTS

This work was supported by the Turkish State Planning Agency (DPT-03K120250) and Bogazici University Scientific Research Projects (BAP-05A601D). The authors also express their gratitude to M. Ipekoglu (for preparing a part of naturally derived HA powders), M.A. Gulgun (for providing SEM analysis), N. Mahmutyazicioglu and C. Baslamisli.

## REFERENCES

- [1] L.L. Hench // *Biomaterials* **19** (1998) 1419.
- [2] P.N. Kumta, C. Sfeir, D. Lee, D. Olton and D. Choi // *Acta Biomaterialia* **1** (2005) 65.
- [3] S.W.K. Kweh, K.A. Khor and P. Cheang // *Journal of Materials Processing Technology* **89** (1999) 373.
- [4] H. Nagai and Y. Nishimura, *US Patent, No: 4330514* (1980).
- [5] F.J.Garcia-Sanz, M.B. Mayor, J.L. Arias, J. Pou, B. Leon and M. Perez-Amor // *Journal of Materials Science: Materials in Medicine* **8** (1997) 861.
- [6] A. Stoch, A. Brozek, G. Kmita, J. Stoch, W. Jastrzebski and A. Rakowska // *Journal of Molecular Structure* **596** (2001) 191.
- [7] O.S. Yildirim, B. Aksakal, H. Celik, Y. Vangolu and A. Okur // *Medical Engineering & Physics* **27** (2005) 221.
- [8] M. Wei, A.J. Ruys, B.K. Milthorpe, C.C. Sorrell and J.H. Evans // *Journal of Sol-Gel Science and Technology* **21** (2001) 39.
- [9] B. Mavis and A.C. Tas // *J. Am. Ceram. Soc.* **83** (2000) 989.
- [10] J. Ma, C. Wang and K.W. Peng // *Biomaterials* **24** (2003) 3505.
- [11] Y. Suda, H. Kawasaki, T. Ohshima, S. Nakashima, S. Kawazoe and T. Toma // *Thin Solid Films* **506** (2006) 115.
- [12] M. Wei, A.J. Ruys, B.K. Milthorpe and C.C. Sorrell // *Journal of Materials Science: Materials in Medicine* **16** (2005) 319.
- [13] M. Ipekoğlu and S. Altintas, In: *ICCE-12, Proceedings CD-ROM, Section: Chemistry of Composites, August 1-6, (2005), Tenerife, Spain.*
- [14] S. Goren, H. Gokbayrak and S. Altintas // *Key Engineering Materials* **264** (2004) 1949.
- [15] I. Zhitomirsky and L. Gal-Or // *Journal of Materials Science: Materials in Medicine* **8** (1997) 213.
- [16] P. Mondragon-Cortez and G. Vargas-Gutierrez // *Materials Letters* **58** (2004) 1336.
- [17] C. Wang, J. Ma, W. Cheng and R. Zhang // *Materials Letters* **57** (2002) 99.